Computational Materials Science 198 (2021) 110715

Contents lists available at ScienceDirect

Computational Materials Science

journal homepage: www.elsevier.com/locate/commatsci

Computational insight on molecular-network disproportionality in over-stoichiometric As_xS_{100-x} nanoarsenicals ($57 < x < 67$)

Oleh Shpotyuk [a,b], Malgorzata Hyla [a], Yaroslav Shpotyuk [c,d,*], Valentina Balitska [e], Vitaliy Boyko [b]

[a] Jan Dlugosz University, 13/15, Al. Armii Krajowej, Czestochowa 42200, Poland
[b] O.G. Vlokh Institute of Physical Optics, 23, Dragomanov Str., Lviv 79005, Ukraine
[c] Ivan Franko National University of Lviv, 1, Universytetska Str., Lviv 79000, Ukraine
[d] Institute of Physics, University of Rzeszow, 1, Pigonia Str., Rzeszow 35-959, Poland
[e] Lviv State University of Life Safety, 35, Kleparivska Str., Lviv 79007, Ukraine

ARTICLE INFO

Keywords:
Nanostructurization
Arsenicals
Disproportionality
Decomposition
Amorphization, *ab-initio* quantum-chemical model
Molecular cluster
Network cluster
Realgar
Dimorphite

ABSTRACT

Competitive pathways of nanostructurization-driven molecular-network disproportionality due to decomposition of dimorphite-type As_4S_3 phase were identified in over-stoichiometric As_xS_{100-x} arsenicals ($57 < x < 67$) employing computational approach based on *ab-initio* quantum-chemical modeling code (CINCA). At the basis of calculated cluster-forming energies, it was proved that amorphization related to direct transformation of dimorphite-type As_4S_3 molecules having *triangle*-like conformation in their network-forming derivatives was dominated in nanoarsenicals within As_4S_4–As_4S_3 cut-section ($50 < x < 57$), while it was unfavorable in more As-rich alloys taken from As_4S_3–As_4S_2 cut-section ($57 < x < 67$). In the latter case, nanostructurization-driven disproportionality attained purely *molecular* character, being governed by indirect decomposition of dimorphite-type As_4S_3 molecules in realgar-type β-As_4S_4 phase supplemented by amorphous a-As_4S_2 substance. Complete hierarchy of molecular-network transformations contributing to this decomposition was reconstructed, the most favorable conformations of participating molecular entities and their network-forming derivatives being parameterized in terms of respective cluster-forming energies.

1. Introduction

The family of arsenosulphides As_xS_{100-x} (referred to as *arsenicals* in biomedical community [1]) is accepted as typical representatives of canonical glass-forming systems where different structure-conformation tendencies could be realized in dependence on composition, these being competitive network-matrix amorphization (vitrification) and layer-type crystallization at the moderated near-stoichiometric As content ($x \approx 40$), as well as molecular- or network-related crystallization in more As-rich compounds ($x > 50$) [2–8]. Under full saturation of covalent bonding in respect to the Mott's *8-N* rule [4,9], which is permanent feature of chalcogenide compounds allowing their consideration in dependence on average coordination numbers Z (i.e. the number of covalent bonds per atom) [10,11], this binary As_xS_{100-x} system reveals unprecedented glass-forming ability near arsenic sesquisulphide $AsS_{1.5}$ (corresponding to As_2S_3 stoichiometry, $x = 40$). Respectively, glassy arsenic trisulphide As_2S_3 cannot be crystallized even at high temperatures during prolonged thermal treatment [2–5], despite *iso*-compositional mineral orpiment with monoclinic structure [12]. The basic motives of this glass-former, i.e. trigonal $AsS_{3/2}$ pyramids interlinked by -S- atom (so-called corner-shared linking) form ground for under-stoichiometric networks of S-rich arsenosulphides As_xS_{100-x} ($x < 40$) realized owing to polymerization ability of bridging $–S_n–$ chains. Under conventional melt-quenching, stable glass-formers in As_xS_{100-x} system are stretched in Z approaching ~ 2.16 [2], corresponding to composition where competitive S separation-agglomeration processes occur. Within this range of S-rich under-stoichiometric alloys up to As_2S_3 ($Z = 2.40$), this system demonstrates few anomalies revealed as *instability onsets* in network cluster-forming energies [13], which often were speculatively accepted as signatures of intermediate optimally-constrained (rigid but stress-free) topological phases [14].

Controversially, under enlarged As content in arsenosulphides over As_2S_3 stoichiometry ($Z > 2.40$), the network-forming amorphization tendencies rapidly disappear near $Z \sim 2.44$–2.46 on a cost of crystalline

* Corresponding author at: Ivan Franko National University of Lviv, 1, Universytetska Str., Lviv 79000, Ukraine.
E-mail address: yshpotyuk@ur.edu.pl (Y. Shpotyuk).

https://doi.org/10.1016/j.commatsci.2021.110715
Received 23 March 2021; Received in revised form 22 June 2021; Accepted 8 July 2021
Available online 16 July 2021

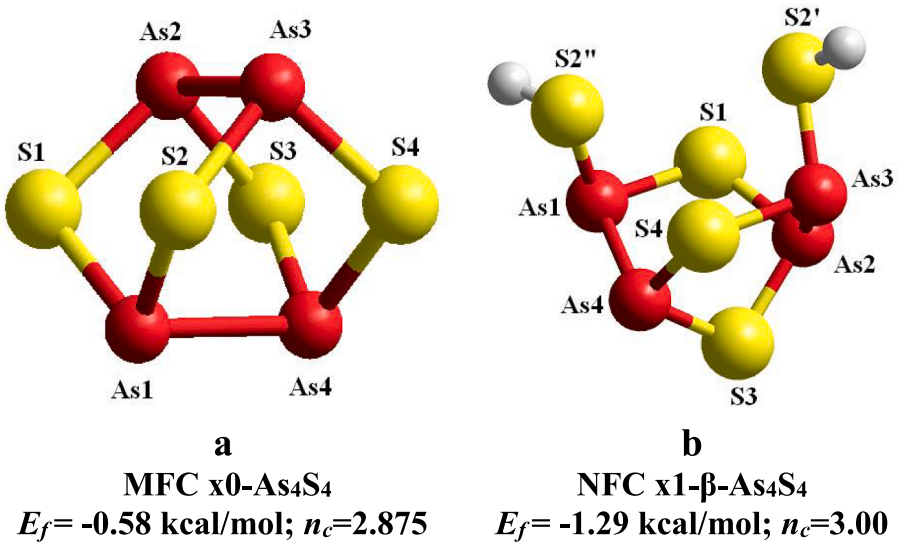

Fig. 1. Geometrically-optimized configurations of realgar-type x0-As_4S_4 MFC (a) and molecular precursor ($As_4S_5H_2$) of x1-β-As_4S_4 NFC derived from x0-As_4S_4 molecule by single x1-breaking in S2 position (b) [36–38]. The S and As atoms are shown by yellow and red balls, respectively, and terminated H atoms are grey-colored. The averaged cluster-forming energies E_f and numbers of topological constraints n_c are given for each cluster. (For interpretation of the references to colour in this figure legend, the reader is referred to the web version of this article.)

conformations involving As_4S_n thioarsenide molecules (with $n = 5, 4, 3$) [2–5,12,15]. These self-closed cage-like molecular entities (having no dangling bonds or terminated inter-cluster links) serve as building blocks for some mineral arsenicals, such as uzonite As_4S_5 ($n = 5$, $Z = 2.46$), realgar α-As_4S_4 ($n = 4$, $Z = 2.50$), bonazitte known as β-As_4S_4 ($n = 4$, $Z = 2.50$), pararealgar As_4S_4 ($n = 4$, $Z = 2.50$), α- and β-dimorphite As_4S_3 ($n = 3$, $Z = 2.57$) [7,12]. The former (As_4S_5) along with tetra-arsenic tetra-sulphide As_4S_4 possessing four crystallographic polymorphs seem most plausible candidates for devitrification in As_xS_{100-x} system in this compositional range ($x > 44$).

Notwithstanding, the phase equilibria in this arsenical system become more complicated with increase in As content, resulting in second glass-forming region within $Z = 2.51–2.66$ range. Hruby [16] was the first who considered these glasses as metastable *plastic* phases with character glass transition temperatures T_g below room temperature. In his opinion, the stable arsenosulphide glasses do not exist in this compositional domain. The second glass-forming region in As-S system is superimposed with dimorphite-type phases, thus meaning governing role of As_4S_3 cage-like molecules ($Z = 2.57$). As was found by Chattopadhyay et al. [17] and generalized by Blachnik and Wickel [18], the plastic-crystalline rhombohedral modification of this phase (having space group *R3*), was capable to introduce rotational disorder in these glasses resulting in pronounced molecular-type conformations. This anomaly was ascribed to idealized C_{3v} symmetry of dimorphite-type As_4S_3 molecules in triangular pyramidal arrangement with -S- bridges on three apical edges adjacent to the basal As_3 ring [19–21]. This conclusion was proved by Aitken for ternary $Ge_xAs_yS_{100-x-y}$ glasses with As:Ge ratio reaching 17:1 [22].

There are no stable crystalline polymorphs under higher As content in As_xS_{100-x} system ($x > 57$), apart from mineral duranusite As_4S ($Z = 2.80$) [12]. The attempt of Kyono [23] to ascribe molecular-forming ability to this arsenical occurred to be completely misleading in view of recent finding of Bonazzi et al. [24], showing that not molecular but rather layered conformation was dominated in this As_4S compound. Nevertheless, the deep meaning for this anomaly has been unclear.

At the boundary of As_xS_{100-x} system, the "pure" arsenic (As) is placed, which is unique element forming glassy substances of different densities (4.3–5.2 g/cm^3) in addition to two crystalline allotropes (low-temperature rhombohedral and high-temperature orthorhombic) [25,26]. The latter (the orthorhombic As) has an evident importance in relation to amorphous As in view of close similarity in the respective inter-atomic conformations [25].

This short overview highlights structural-compositional complexity in over-stoichiometric As-rich arsenosulphides ($Z > 2.40$), where principally different inter-atomic arrangements (nanocrystalline and amorphous) are found. This conclusion concerns As_xS_{100-x} arsenicals stretched in chemical compositions above $Z > 2.57$, which possess multiphase equilibria disturbed by thermal-alteration decomposition of dominated dimorphite-type As_4S_3 phase into realgar-type β-As_4S_4 phase supplemented by extraction of unknown amorphous substance [17,18]:

$$2{\cdot}As4S3 \rightarrow \beta - As4S4 + a - (As - S) \quad (1)$$

Assuming that As_4S_4 molecules ($Z = 2.50$) are continuously generated under nanostructurization from dimorphite-type As_4S_3 molecules in an environment of some network-forming remainder (such as caused by high-energy mechanical milling), the composition of the amorphous phase in (1) was hypothesized to approach a-As_4S_2 ($Z = 2.67$) [27,28]. In this work, we try to justify compositional variations in the group of over-stoichiometric As_xS_{100-x} nanoarsenicals ($57 < x < 67$) governed by decomposition reaction (1) employing *ab-initio* quantum-chemical modeling route with atomic cluster-simulation code CINCA (cation-interlinked network cluster approach) [29–31].

2. CINCA modeling of molecular-network conformations in covalent substances

Geometrically-optimized conformations of arsenical cage-like molecules (molecular-forming clusters, MFC) and their network derivatives (network-forming clusters, NFC) participating in disproportionality (1) were simulated using the cluster-modeling algorithm CINCA [13,29–31].

The NFC conformations were reconstructed by breaking respective MFC on a few fragments, linking them with surrounding through common sulfur atoms (considered as sulfur half-atomic $S_{1/2}…S_{1/2}$ bridges) [29]. The meaningful nomenclature for NFC was developed in terms of broken covalent bonding on bridging S atoms using xm- prefix before MFC formula to denote the number of S positions available for such breaking in the parent arsenical molecule (which is marked in this nomenclature as x0-MFC).

The HyperChem Release 7.5 program based on the restricted Hartree-Fock self-consistent field method with split-valence double-zeta basis set and single polarization function 6-311G* [32,33] was used to calculate cluster-forming energy E_f. Geometrical optimization and single-point energy calculations were performed for each cluster configuration with Fletcher-Reeves conjugate gradient method until the root-mean-square gradient of 0.1 kcal/(Å·mol) was reached. In final, the calculated cluster-forming energy E_f was corrected on the energy of

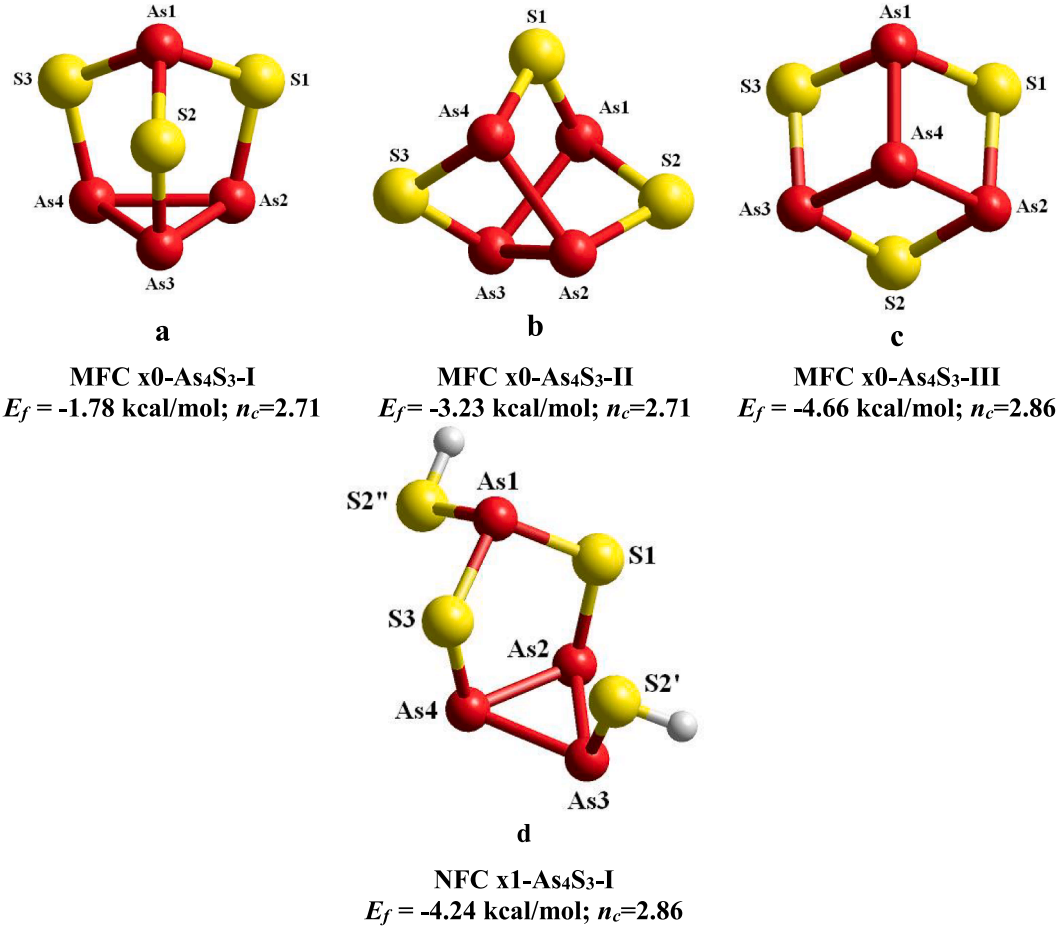

Fig. 2. Geometrically-optimized configurations of dimorphite-type As_4S_3 MFC in *triangle-* (a), *zig-zag chain-* (b) and *star*-like (c) conformations, and molecular precursor ($As_4S_4H_2$) of x1-As_4S_3-I NFC derived from x0-As_4S_3-I molecule by single x1-breaking in S2 position (d). The S and As atoms are shown by yellow and red balls, and terminated H atoms are grey-colored. The averaged cluster-forming energies E_f and numbers of topological constraints n_c are given for each cluster. (For interpretation of the references to colour in this figure legend, the reader is referred to the web version of this article.)

terminated H atoms, transforming the NFC in its molecular precursor (the H-terminated self-consistent MFC) using the route developed elsewhere [29,34,35]. For a sake of convenience, the E_f energy was recalculated respectively to the energy of basic glass-forming structural unit in As_xS_{100-x} thioarsenides, which is single trigonal $AsS_{3/2}$ pyramid (−79.404 kcal/mol [13]). Ascribing stretching and bending forces to covalent bonds in arsenicals, the average number of topological constraints per atom n_c was defined for each cluster configuration in respect to the Phillips-Thorpe constraint-counting algorithm [10,11].

Thus, the developed *ab-initio* quantum-chemical cluster-modeling algorithm (CINCA) [13,29–31] allows quantitative comparison of atomic-structural transformations related to MFC and NFC at the basis of calculated cluster-forming energies E_f, parameterizing adequately competitive interphase crystallization-amorphization scenarios in covalent-bonded substances like arsenicals. These transitions can be visualized on reconstructed potential energy landscapes showing variety of network-forming amorphization states originated from parent arsenical cage-like molecules in multi-well presentation respectively to the calculated E_f energies

3. Results and discussion

To understand the nature of interphase disproportionality occurring in the group of over-stoichiometric As-rich As_xS_{100-x} nanoarsenicals ($Z > 2.57$), the most plausible molecular-to-network microstructural transformations should be reconstructed for molecular As_4S_n thioarsenides [15] participating in the decomposition reaction (1), these being as follows realgar-type As_4S_4 (n = 4, $Z = 2.50$), dimorphite-type As_4S_3 (n = 3, $Z = 2.57$) and As_4S_2 (n = 2, $Z = 2.67$).

3.1. Molecular-network conformations related to realgar-type As_4S_4 thioarsenides ($Z = 2.50$)

The quantum-chemical model of realgar-type As_4S_4 molecule was developed in our preliminary research [36]. This cage-like molecule shown on Fig. 1a (x0-As_4S_4 in nomenclature of broken covalent bonding) possessing D_{2d} symmetry is composed of eight heteronuclear As-S bonds and two homonuclear As-As bonds in mutually orthogonal arrangement, evolving eight small rings (four pentagons and four hexagons), thus resulting in under-constrained structural motive with $n_c = 2.875$ (less than space dimensionality, $D = 3$). The calculated cluster-forming energy E_f for this molecule (in respect to the energy of single $AsS_{3/2}$ pyramid [13]) equals −0.58 kcal/mol, this value being dominated over all thioarsenide As_4S_n molecules in over-stoichiometry region ($Z > 2.50$) [37].

Topological variants of amorphization scenarios related to NFC derived from x0-As_4S_4 MFC were computed in [37,38]. In practice, because of low barrier of room-temperature realgar α-As_4S_4 phase transition to high-temperature β-As_4S_4 phase [38], all NFC are stabilized from β-As_4S_4 phase (so this molecule participating in nanostructurization can be reasonably nominated as x0-β-As_4S_4). The smallest $E_f = -1.29$ kcal/mol is achieved for single-broken NFC (x1-β-As_4S_4) derived from its H-terminated molecular precursor $As_4S_5H_2$ shown on Fig. 1b [37,38]. This NFC having one hexagon and two

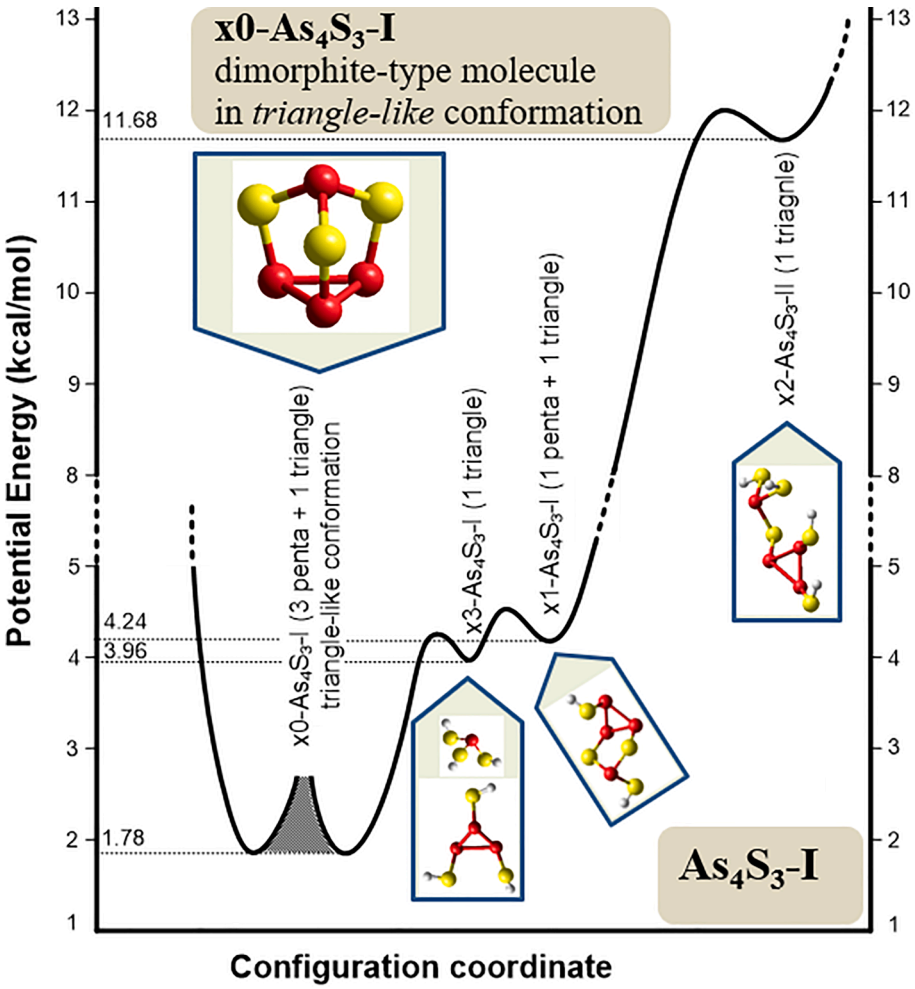

Fig. 3. Potential energy landscapes showing diversity of amorphizing NFC-related states originated from dimorphite-type x0-As_4S_3-I molecule possessing *triangle*-like conformation. The double-well presentation of ground state for x0-As_4S_3-I molecule corresponds to low- and high-temperature modifications of tetra-arsenic trisulphide after Whitfield [47,48]. The geometrically-optimized configurations of H-terminated molecular precursors derived from this x0-As_4S_3-I molecule by multi-breaking in respective S atom positions are depicted. The settle-points ascribed to the NFC (keeping small rings, such as triangles and pentagons nominated in parenthesis) are pointed out with cluster-forming energies E_f given on potential energy axis (see text for more details).

pentagons in the nearest inter-atomic arrangement is optimally-constrained since $n_c = 3.00$. Therefore, amorphous structures bult of such NFC are most favorable. Because of low barrier with ground state of parent x0-β-As_4S_4 molecule ($\Delta E_f = 0.71$ kcal/mol), the expected molecular-to-network transition occurs even in directly synthesized arsenic monosulphide (AsS), being a source of its spontaneous amorphization [39–41]. Other alternative pathways for solid state amorphization from realgar-type β-As_4S_4 phase are less possible in view of unfavorable energetic barriers ΔE_f [38].

3.2. Network conformations derived from dimorphite-type As_4S_3 molecules

In general, there are three topologically different conformations for cage-like As_4S_3 molecule in dependence on the arrangement of three homonuclear As-As covalent bonds as depicted on Fig. 2, these being *triangle*-like (due to basal As_3-ring built of As2-As3-As4 atoms surmounted by $AsS_{3/2}$ pyramid, see Fig. 2a), *chain*-like (due to three As-As bonds in *zig-zag* sequence of four As atoms As1-As3-As2-As4, see Fig. 2b) and *star*-like (due to three As-As bonds having the same origin on As4 atom, see Fig. 2c). The optimized geometries of these As_4S_3 MFC were simulated previously by Kyono [23], but this author was failed to distinguish most favorable conformations among these As_4S_3 clusters.

In respect to E_f energies calculated using the CINCA modelling algorithm, the most plausible is x0-As_4S_3-I MFC possessing *triangle*-like configuration for three neighboring As-As bonds having $E_f = -1.78$ kcal/mol (Fig. 2a). The idealized geometry of this MFC possessing C_{3v} symmetry with all seven atoms positioned on the same surrounding sphere and forming four small rings (three pentagons and one triangle) was analyzed in details elsewhere [18–20]. From purely topological viewpoint, this cage-like molecule is under-constrained because of $n_c = 2.71$ (which is evidently less than space dimensionality $D = 3$). This *triangle*-like MFC (x0-As_4S_3-I) is typical for mineral As_4S_3 polymorphs (α/β-dimorphites) [42,43].

Other cage-like As_4S_3 MFC are unfavorable as compared with *triangle*-like x0-As_4S_3-I molecule on Fig. 2a. The calculated cluster-forming energy E_f approaches −3.23 kcal/mol for *chain*-like As_4S_3 molecule (x0-As_4S_3-II, Fig. 2b) and −4.66 kcal/mol for *star*-like molecule (x0-As_4S_3-III, Fig. 2c). This finding is in excellent agreement with absence of As_4S_3 modifications possessing homonuclear As-As bonding in such arrangements. Therefore, in the further consideration concerning molecular-network conformations in these As_4S_3-rich arsenicals, we are concentrated on dimorphite-type MFC (x0-As_4S_3-I) with three As-As bonds forming triangle.

The dimorphite-type As_4S_3 MFC allows three different NFC configurations which can be reconstructed from the parent *triangle*-like x0-As_4S_3-I molecule by single-, double- or triple-breaking in available S atom positions.

In respect to our calculations, the most plausible is NFC originated from x0-As_4S_3-I molecule due to single x1-breaking in S2 position (Fig. 2d) keeping two neighboring small rings, these being (As2As3As4) triangle composed of three As-As bonds and (As2As4S3As1S1) pentagon adjusted to this triangle. This x1-As_4S_3-I NFC having $E_f = -4.24$ kcal/mol is principal "building unit" in the reconstruction of under-constrained amorphous network with $n_c = 2.86$.

The similar cluster-forming energy ($E_f = -3.96$ kcal/mol) is character

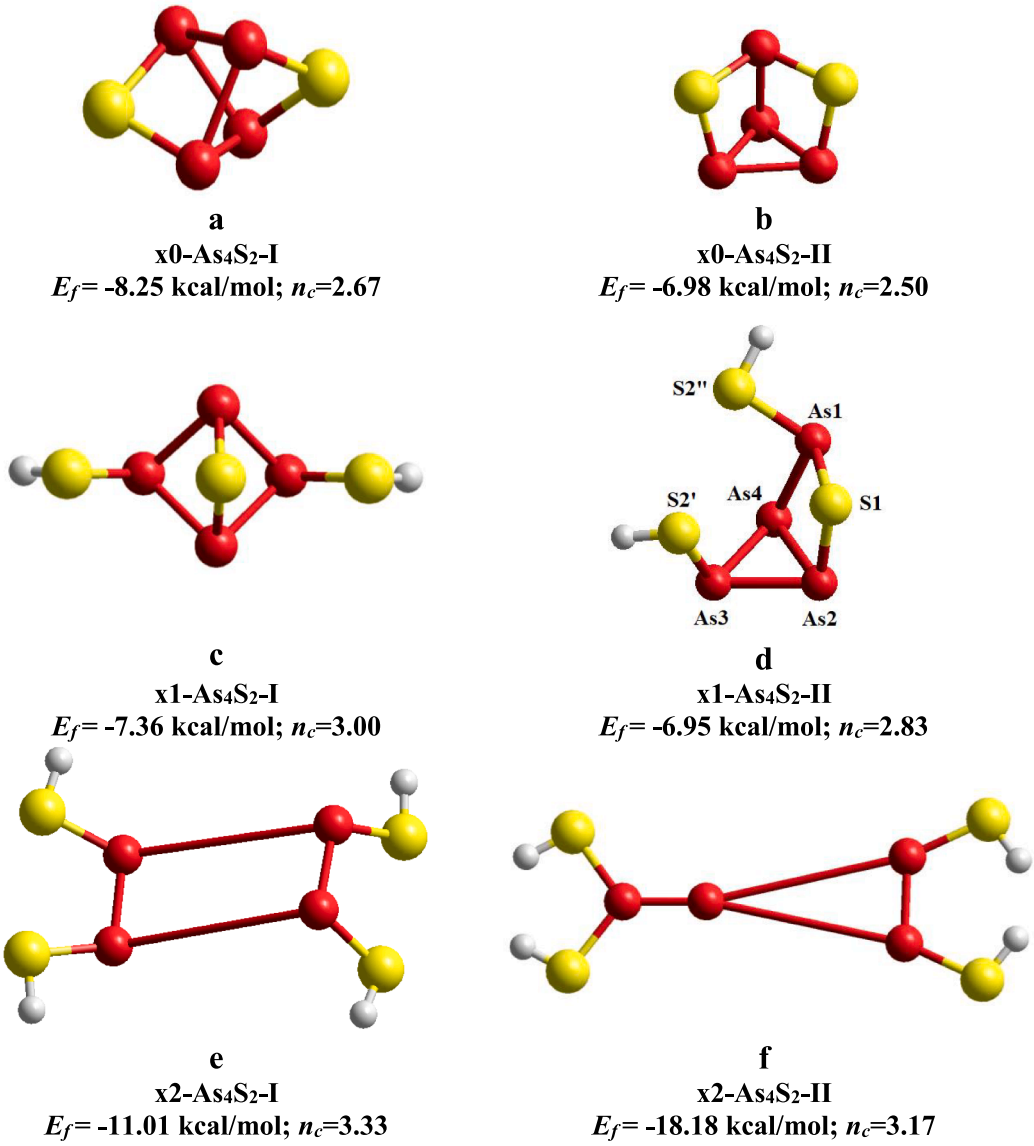

Fig. 4. Geometrically-optimized configurations of cage-like As_4S_2 MFC in *chain*-like (a) and *star-triangle*-like (b) geometries, and H-terminated molecular precursors of NFC derived from these molecules by single-breaking (x1-As_4S_2-I – c; x1-As_4S_2-II – d) and double-breaking (x2-As_4S_2-I – e; x2-As_4S_2-II – f) in S atom positions. The S and As atoms are shown by yellow and red balls, and terminated H atoms are grey-colored. The averaged cluster-forming energies E_f and numbers of topological constraints n_c are given for each cluster. (For interpretation of the references to colour in this figure legend, the reader is referred to the web version of this article.)

for optimally-constrained NFC derived from x0-As_4S_3-I molecule by triple x3-breaking in all S atom positions (not shown on Fig. 2). In fact, this x3-As_4S_3-I NFC initiates network separation on two optimally-constrained sub-networks based on $AsS_{3/2}$ trigonal pyramids (Z = 2.40, n_c = 3.00) and S-terminated As_3-triangles (i.e. $As_3S_{3/2}$ clusters with Z = 2.67 and n_c = 3.00). Such transition can be considered as continuation of original amorphization process initiated by single x1-breaking in the parent x0-As_4S_3-I molecule, which occurs rather in As_4S_3 ("pure" dimorphite-type As_4S_3 structures, Z = 2.57) with low barrier of molecular-to-network transition ΔE_f = (4.24–1.78) kcal/mol = 2.46 kcal/mol, as evidenced from potential energy landscape on Fig. 3.

In contrast, the optimally-constrained (n_c = 3.00) NFC derived from x0-As_4S_3-I molecule due to double ×2-breaking (double-broken x2-As_4S_3-I NFC) keeping one small ring (As_3-triangle) cannot be stabilized in the realistic arsenical structures in view of very unfavorable cluster-forming energy E_f = −11.68 kcal/mol (see Fig. 3).

3.3. Network conformations expected for cage-like As_4S_2 molecules

It is known that As_4S_n thioarsenides do not form stable molecular entities with n = 2 [15], as it also follows from results of the current quantum-chemical modeling. However, *iso*-compositional (As_4S_2) network configurations can be considered as quite competitive in over-stoichiometric arsenosulphides (Z > 2.50) under inter-crystalline transformations complemented by solid state amorphization processes [40,41].

In principle, two structural configurations of cage-like As_4S_2 molecule are possible, which can be derived from the respective dimorphite-type As_4S_3 MFC by removing one of S atoms [23].

The first MFC (x0-As_4S_2-I) appears when S atom is removed from one of -S-bridges terminated the pairs of directly non-bonded As atoms within As1-As3-As2-As4 sequence in *zig-zag* (*chain*-like) conformation of As_4S_3 MFC (x0-As_4S_3-II molecule shown on Fig. 2b), or within As4-As_3 star in *star*-like As_4S_3 MFC (x0-As_4S_3-III molecule shown on Fig. 2c). The second MFC (x0-As_4S_2-II) appears when S atom is removed from one of -S-atom bridges on apical edges adjacent to the basal As_3 ring in *triangle*-

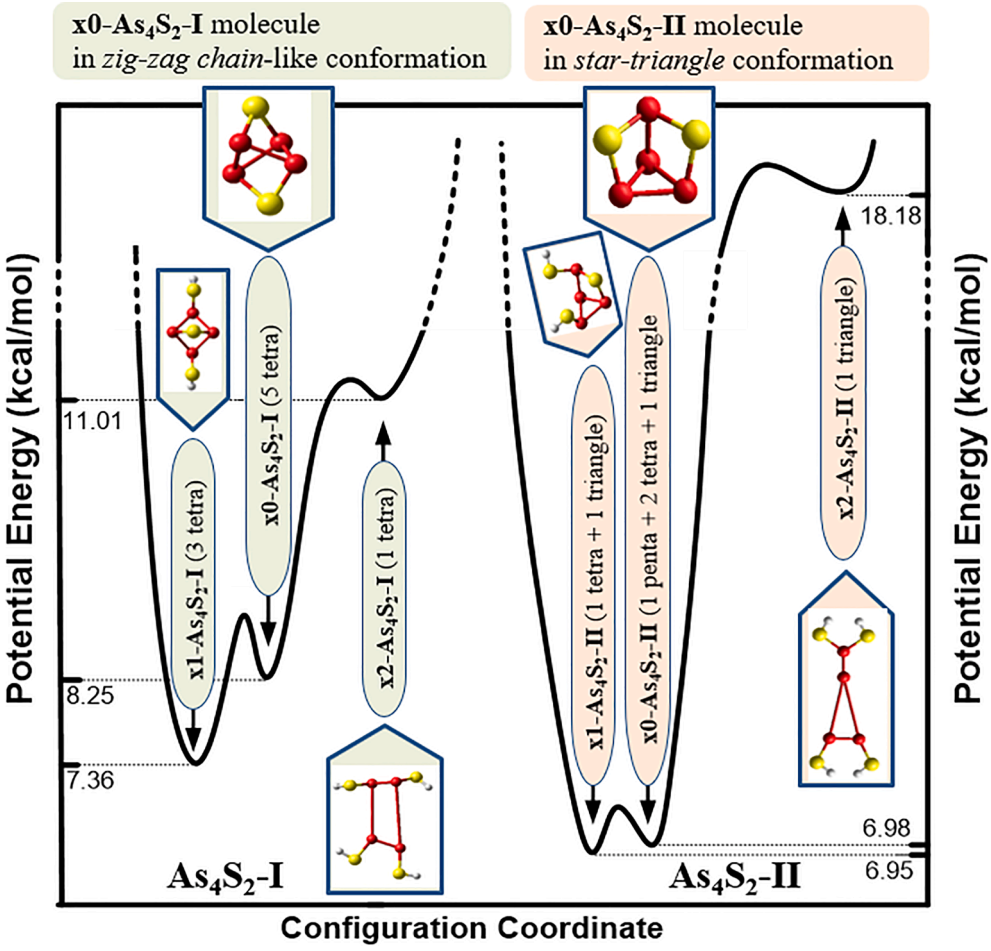

Fig. 5. Potential energy landscapes showing diversity of amorphizing NFC-related states originated from As_4S_2-type MFC possessing *zig-zag chain*-like (x0-As_4S_2-I, at the left) and *star-triangle*-like (x0-As_4S_2-II, at the right) conformations. The geometrically-optimized configurations of H-terminated molecular precursors derived from these molecules by multi-breaking in respective S atom positions are depicted. The settle-points ascribed to the NFC (keeping small rings, such as triangles and pentagons nominated in parenthesis) are pointed out with cluster-forming energies E_f given on potential energy axis (see text for more details).

Table 1
Geometrically-optimized bond distances d and angles α in single-broken NFC x1-As_4S_2-II derived from cage-like As_4S_2 MFC in *star-triangle*-like geometry (the atom labels refer to Fig. 4d).

Bond distances		Bond angles	
Atoms	d, Å	Angle	α, °
Direct bonded distances		∠ **S-As-S**	
As1 – As4	2.4652	∠ **S1-As1-S2″**	105.704
As2 – As3	2.4390		
As2 – As4	2.4964	∠ **S-As-As**	
As3 – As4	2.4627	∠ **S1-As1-As4**	91.535
As1 – S1	2.2694	∠ **S2″-As1-As4**	105.070
As1 – S2″	2.2519	∠ **S1-As2-As4**	90.690
As2 – S1	2.2712	∠ **S2′-As3-As4**	111.076
As3 – S2′	2.2471	∠ **S1-As2-As3**	101.069
Non-bonded distances		∠ **S2′-As3-As2**	104.642
As1 – As2	3.2694		
As1 – As3	3.9671	∠ **As-S-As**	
As1 – S2′	4.1315	∠ **As1-S1-As2**	92.117
As2 – S2′	3.7107		
As2 – S2″	4.8576	∠ **As-As-As**	
S1 – S2′	3.5445	∠ **As3-As2-As4**	59.851
As3 – S1	3.6379	∠ **As2-As3-As4**	60.232
As3 – S2″	4.5085	∠ **As2-As4-As3**	58.917
As4 – S1	3.3952	∠ **As1-As4-As2**	82.435
As4 – S2′	3.8852	∠ **As1-As4-As3**	107.227
As4 – S2″	3.7463		
S1 – S2″	3.6038		

like MFC (x0-As_4S_3-I molecule shown on Fig. 2a). The optimal geometries of these *chain*-like (x0-As_4S_2-I) and *star-triangle*-like (x0-As_4S_2-II) MFC identified with CINCA modeling are respectively presented on Fig. 4a and b. These MFC are under-constrained ($n_c < 3.00$) in view of great number of small rings in both geometries (five tetragons in x0-As_4S_2-I MFC on Fig. 4a, and one pentagon, two tetragons and one triangle in x0-As_4S_2-II MFC on Fig. 4b).

The NFC can be derived from these As_4S_2 MFC by single- or double-breaking in available S atom positions, the respective optimized configurations of these NFC being reproduced on Fig. 4c–f. The both NFC derived by double-breaking are unfavorable in view of extra-high stretching distortions in the remaining small rings (tetragon on Fig. 4e, and triangle on Fig. 4f). However, the NFC produced by single-breaking are more favorable as compared even with parent As_4S_2 MFC from which they were derived (Fig. 4c and d).

Noteworthy, the cluster-forming energy E_f = -6.95 kcal/mol obtained for under-constrained ($n_c = 2.83$) single-broken x1-As_4S_2-II NFC is dominated among energies of all As_4S_2-type clusters (MFC and NFC), thus defining preferential direction in network-forming structural transformations expected in the respective arsenicals (as it illustrated on Fig. 5 by the lowest well on potential energy landscapes). The geometrically-optimized equivalent bond distances d and angles α in this NFC derived from cage-like As_4S_2 MFC in *star-triangle*-like geometry are gathered in Table 1. The optimized direct As-As distances ($d \sim 2.466$ Å) and α angles on As atoms (∠As-As-As) within basal As_3 ring in this NFC slightly deviate around equilibrium values found in the Kyono's models [42] for *star-triangle*-like As_4S_2 molecule ($d = 2.466$ Å, $\alpha = 60.00°$) or As_4S_3 molecule in *triangle*-like geometry ($d = 2.465$ Å $\alpha = 60.00°$)). The averaged direct As-S bond distances are close to the length of

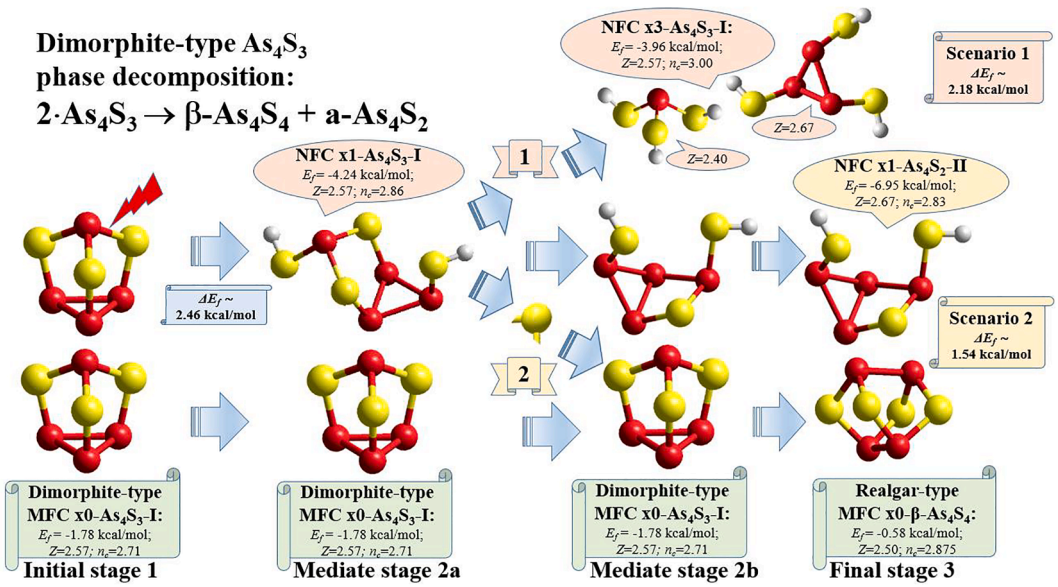

Fig. 6. Disproportionality pathways in over-stoichiometric As_xS_{100-x} arsenicals related to *direct* decomposition of *triangle*-like dimorphite-type As_4S_3 MFC in two optimally-constrained NFC with $Z = 2.40$ and $Z = 2.67$ (scenario 1) and *indirect* decomposition in realgar-type β-As_4S_4 phase supplemented by network-forming amorphous a-As_4S_2 substance (scenario 2). The geometrically-optimized configurations of MFC and NFC are reproduced with S and As atoms labeled by yellow and red balls, and terminated H atoms are grey-colored. The energetic barriers ΔE_f to be overcome for these disproportionality scenarios, average values of coordination numbers Z, cluster-forming energies E_f and numbers of topological constraints n_c are given (see text for more details). (For interpretation of the references to colour in this figure legend, the reader is referred to the web version of this article.)

heteronuclear As-S covalent bond in amorphous arsenosulphides [2–7,19,21]. The same concerns the averaged non-bonded As-As and As-S distances and bond angles α, which determine stable under-constrained amorphous network ($n_c = 2.83$) derived from destroyed x1-broken As_4S_2 MFC.

3.4. Molecular-network disproportionality activated in As_xS_{100-x} nanoarsenicals ($57 < x < 67$)

Competitive nanostructurization-driven disproportionality in over-stoichiometric As_xS_{100-x} arsenicals is related to *direct* decomposition of *triangle*-like dimorphite-type As_4S_3 cage molecules (such as *triangle*-like x0-As_4S_3-I MFC, $n_c = 2.71$) to their most energetically favorable network-forming derivatives (NFC such as under-constrained x1-As_4S_3-I, $n_c = 2.86$, or optimally-constrained x3-As_4S_3-I, $n_c = 3.00$) depicted as scenario 1 on Fig. 6. To be realized, these transformations need overcoming potential energy barrier ΔE_f approaching difference in respective cluster-forming energies (2.46 kcal/mol for x1-As_4S_3-I, or 2.18 kcal/mol for x3-As_4S_3-I, see Fig. 3). Interestingly, if the above transition to optimally-constrained network with $n_c = 3.00$ prevails, the generated amorphous phase occurs to be intrinsically decomposed on two optimally-constrained sub-networks (the stoichiometric, $Z = 2.40$, and over-stoichiometric, $Z = 2.67$). It was shown recently this *direct* molecular-network disproportionality was indeed dominated in As_xS_{100-x} nanoarsenicals taken within As_4S_4–As_4S_3 cut-section compositionally corresponding to $50 < x < 57$ [27,28].

The character of structural transformations induced by nanostructurization is cardinally changed in the case of over-stoichiometric As_xS_{100-x} nanoarsenicals above As_4S_3 composition ($Z > 2.57$), i.e. in compositional domain where dimorphite-type As_4S_3 cage-like molecules obeying *triangle*-like conformation (x0-As_4S_3-I MFC, $Z = 2.57$) are diluted in more As-rich network with $Z > 2.57$, the respective initiation and propagation stages of this *indirect* molecular-network disproportionality scenario 2 being illustrated on Fig. 6. Nanostructurization-driven transformations in these arsenicals attain purely *molecular* character, stabilizing most energetically favorable conformations of participating MFC and their network-forming derivatives.

The decomposition beginning is triggered by destruction of one of dimorphite-type As_4S_3 MFC shown on Fig. 2a (possessing $E_f = -1.78$ kcal/mol) due to breaking one of its intramolecular bonds (at the initial stage 1, see Fig. 6). This over-barrier transition results (at the mediate stage 2a, see Fig. 6) in single-broken NFC x1-As_4S_3-I having $E_f = -4.24$ kcal/mol (reproduced on Fig. 2d) as the most energetically favorable remainder of this just-destructed dimorphite-type As_4S_3 molecule:

$$x0 - As_4S_3 - I \rightarrow x1 - As_4S_3 - I + (\Delta E_f = +2.46 kcal/mol) \quad (2)$$

The above reaction (2) is followed by release of one distinct S atom away from the destructed x0-As_4S_3-I MFC, transforming it to the most favorable x1-As_4S_2-II NFC having $E_f = -6.95$ kcal/mol (reproduced in Fig. 4d).

This discrete S atom can be considered as elementary *chain*-like NFC composed of two sulfur half-atoms $S_{1/2}$…$S_{1/2}$ [29], possessing cluster-forming energy $E_f = -65.63$ kcal/mol in an absolute determination [31], which is equivalent to $E_f = -13.77$ kcal/mol as determined in respect to single $AsS_{3/2}$ pyramid. Thereby, at the mediate stage 2b (see Fig. 6), these microstructural changes occur as transitions over energetic barrier approaching $\Delta E_f = 3.68$ kcal/mol:

$$x1 - As_4S_3 - I \rightarrow x1 - As_4S_2 - II + S_{2/2} + (\Delta E_f = +3.68 kcal/mol) \quad (3)$$

At the final stage 3 (Fig. 6), this S atom interacts with neighboring dimorphite-type As_4S_3 MFC transforming it in realgar-type x0-As_4S_4 MFC having $E_f = -0.58$ kcal/mol (reproduced in Fig. 1a), this intermolecular transformation being energetically favorable because of negative ΔE_f:

$$S_{2/2} + x0 - As_4S_3 - I \rightarrow x0 - As_4S_4 + (\Delta E_f = -2.70 kcal/mol) \quad (4)$$

Composing all stages of the above molecular-network transformations obeying reactions (2)–(4), one gets finally the overall decomposition scenario 2 in over-stoichiometric As_xS_{100-x} arsenicals ($57 < x < 67$) occurring with positive energetic barrier $\Delta E_f = 1.54$ kcal/mol:

$$2{\cdot}x0 - As_4S_3 - I \rightarrow x1 - As_4S_2 - II + x0 - \beta - As_4S_4 \rightarrow \beta - As_4S_4 + a - As_4S_2 + (\Delta E_f = +1.53 kcal/mol) \quad (5)$$

This *indirect* disproportionality (corresponding to scenario 2 on Fig. 6) is more favorable (in view of inter-well barrier ΔE_f reduced on 0.64 kcal/mol) as compared with *direct* decomposition of dimorphite-type x0-As_4S_3-I molecule in its network-forming derivatives (scenario 1 on Fig. 6).

4. Conclusions

Competitive scenarios of nanostructurization-driven molecular-network disproportionality governed by direct and indirect decomposition of dimorphite-type As_4S_3 phase were identified in over-stoichiometric As_xS_{100-x} arsenicals ($57 < x < 67$) employing *ab-initio* quantum-chemical simulation code (CINCA). At the basis of calculated cluster-forming energies, it was proved that amorphization related to *direct* transformation of dimorphite-type As_4S_3 molecules possessing *triangle*-like conformation to their network-forming derivatives was dominated in arsenicals within As_4S_4–As_4S_3 cut-section nearby As_4S_3 composition ($x = 57$), while it was energetically unfavorable in more As-rich arsenosulphides from As_4S_3–As_4S_2 cut-section ($57 < x < 67$). In the latter case, nanostructurization-driven disproportionality attains purely *molecular* character, being governed by *indirect* decomposition of dimorphite-type As_4S_3 molecules in realgar-type β-As_4S_4 phase and amorphous a-As_4S_2 substance with network structure. Complete hierarchy of molecular-network structural transformations contributing to the above decomposition was reconstructed, and energetically favorable conformations of participating molecular entities and their network-forming derivatives were justified in terms of cluster-forming energies.

5. Data availability

Data will be made available on request.

CRediT authorship contribution statement

Oleh Shpotyuk: Conceptualization, Supervision, Validation, Writing - original draft. **Malgorzata Hyla:** Data curation, Formal analysis, Visualization. **Yaroslav Shpotyuk:** Data curation, Formal analysis, Writing - review & editing. **Valentina Balitska:** Writing - review & editing, Formal analysis, Visualization. **Vitaliy Boyko:** Data curation, Validation, Visualization.

Declaration of Competing Interest

The authors declare that they have no known competing financial interests or personal relationships that could have appeared to influence the work reported in this paper.

Acknowledgements

The paper is part of scientific research performed within the project No 0119U100357, subject of Scientific Program funded by Ministry of Education and Science of Ukraine (2019-2022).

References

[1] P.J. Dilda, P.J. Hogg, Arsenical-based cancer drugs, Cancer Treat. Rev. 33 (6) (2007) 542–564, https://doi.org/10.1016/j.ctrv.2007.05.001.
[2] Z.U. Borisova, Chemistry of glassy semiconductors, Ed. Leningrad. Univ., Leningrad, 1972, 247 p. (in rus.).
[3] Z.U. Borisova, Glassy Semiconductors, Plenum Press, New York, 1981, 505 p.
[4] A. Feltz, Amorphous Inorganic Materials and Glasses, Weinheim / VCH Publishers, New York, VCH Verlagsgesellschaft, 1993, p. 446.
[5] G.Z. Vinogradova, Glass formation and phase equilibria in chalcogenide systems. Binary and ternary systems (in Rus.), Nauka, Moscow, (1984).
[6] M. Popescu, Non-crystalline chalcogenides, Kluwer Academic Publ., Dordrecht-Boston-London (2000).
[7] A.L. Emelina, A.S. Alikhanian, A.V. Steblevskii, E.N. Kolosov, Phase diagram of the As-S system, Inorg. Mater. 43 (2) (2007) 95–104, https://doi.org/10.1134/S002016850702001X.
[8] Chalcogenide glasses: Preparation, properties and applications. Woodhead Publishing Series in Electronics and Optical Materials, J.-L. Adam, X. Zhang (Eds.) Philadelphia-New Delhi (2013).
[9] N.F. Mott, E.A. Davis, Electron Processes in Non-Crystalline Materials, –, Clarendon Press, Oxford, 1979, p. 663 p..
[10] J.C. Phillips, Topology of covalent non-crystalline solids. I: Short-range order in chalcogenide alloys, J. Non-Cryst. Solids 34 (2) (1979) 153–181, https://doi.org/10.1016/0022-3093(79)90033-4.
[11] M.F. Thorpe, Continuous deformations in random networks, J. Non-Cryst. Solids 57 (3) (1983) 355–370, https://doi.org/10.1016/0022-3093(83)90424-6.
[12] P. Bonazzi, L. Bindi, A crystallographic review of arsenic sulfides: effects of chemical variations and changes induced by exposure to light, Z. Ktistallogr. 223 (2008) 132–147, https://doi.org/10.1524/zkri.2008.0011.
[13] Shpotyuk O., Hyla M. Compositionally-dependent network-forming tendencies in S-rich As-S glasses. – J. Optoelectron. Adv. Mater. 19 (2017) 48-56. https://joam.inoe.ro/articles/compositionally-dependent-network-forming-tendencies-in-s-rich-as-s-glasses/.
[14] P. Chen, C. Holbrook, P. Boolchand, D.G. Georgiev, K.A. Jackson, M. Micoulaut, Intermediate phase, network demixing, boson and floppy modes, and compositional trends in glass transition temperatures of binary As_xS_{1-x} system. –, 224208–1-224208-15, Phys. Rev. B 78 (2008), https://doi.org/10.1103/PhysRevB.78.224208.
[15] G.V. Gibbs, A.F. Wallace, R.T. Downs, N.L. Ross, D.F. Cox, K.M. Rosso, Thioarsenides: a case for long-range Lewis acid-base-directed van der Waals interactions, Phys. Chem. Minerals 38 (4) (2011) 267–291, https://doi.org/10.1007/s00269-010-0402-3.
[16] A. Hruby, A study of glass-forming ability and phase diagram of the As-S system, J. Non-Cryst. Solids 28 (1978) 139–142, https://doi.org/10.1016/0022-3093(78)90080-7.
[17] T.N. Chattopadhyay, E. Gmelin, H.G. von Schnering, Heat capacity of the phase transitions in As_4S_4 and As_4S_4. – Phys, Stat. Sol. A 76 (1983) 543–551, https://doi.org/10.1002/pssa.2210760217.
[18] R. Blachnik, U. Wickel, Thermal behavior of A_4B_3 cage molecules (A = P, As; B = S, Se), Thermochim. Acta 81 (1984) 185–196, https://doi.org/10.1016/0040-6031(84)85123-0.
[19] T.J. Bastow, I.D. Campbell, H.J. Whitfield, An arsenic-75 nuclear quadruple resonance study of α and β As_4S_3. –, Aust. J. Chem. 25 (1972) 2291–2299, https://doi.org/10.1071/CH9722291.
[20] S. Soyer-Uzun, S. Sen S., B.G. Aitken, Network vs molecular structural characteristics of Ge-doped arsenic sulfide glasses: A combined neutron/X-ray diffraction, extended X-ray absorption fine structure, and Raman spectroscopic study, J. Phys. Chem. C113 (2009) 6231-6242. doi: 10.1021/jp810446g.
[21] A.C. Wright, B.G. Aitken, G. Cuello, R. Haworth, R.N. Sinclair, J.R. Stewart, J. W. Taylor, Neutron studies of an inorganic plastic glass, J. Non-Cryst. Solids 357 (14) (2011) 2502–2510, https://doi.org/10.1016/j.jnoncrysol.2010.12.054.
[22] B.G. Aitken, GeAs sulfide glasses with unusually low network connectivity, J. Non-Cryst. Solids 345–346 (2004) 1–6, https://doi.org/10.1016/j.jnoncrysol.2004.07.036.
[23] A. Kyono, Ab initio quantum chemical investigation of arsenic sulfide molecular diversity from As_4S_6 and As_4, Phys. Chem. Minerals 40 (9) (2013) 717–731, https://doi.org/10.1007/s00269-013-0607-3.
[24] P. Bonazzi, G.O. Lepore, L. Bindi, Molecular *versus* layered structure in arsenic sulphide minerals: the case of duranusite, As_4S, Eur. J. Mineral. 28 (1) (2016) 147–151, https://doi.org/10.1127/ejm/2015/0027-2474.
[25] P.M. Smith, A.J. Leadbetter, A.J. Apling, The structures of orthorhombic and vitreous arsenic, Phil. Mag. 31 (1) (1975) 57–64, https://doi.org/10.1080/14786437508229285.
[26] Greaves G.N., Elliott S.R., Davei E.A. Amorphous arsenic. – Adv. Phys. 28 (1979) 49-141. doi: 10.1080/00018737900101355.
[27] O. Shpotyuk, P. Demchenko, Y. Shpotyuk, S. Kozyukhin, A. Kovalskiy, A. Kozdras, Z. Lukáčová Bujňáková, P. Baláž, Milling-driven nanonization of As_xS_{100-x} alloys from second glass-forming region: The case of higher-crystalline arsenicals (51<x<56), 120086–1-12, J. Non-Cryst. Solids 539 (2020), https://doi.org/10.1016/j.jnoncrysol.2020.120086.
[28] O. Shpotyuk, S. Kozyukhin, P. Demchenko, Y. Shpotyuk, A. Kozdras, M. Vlcek, A. Kovalskiy, Z. Lukáčová Bujňáková, P. Baláž, V. Mitsa, M. Veres, Milling-driven nanonization of As_xS_{100-x} alloys from second glass-forming region: The case of lower-crystalline arsenicals (56<x<66), 120339–1-12, J. Non-Cryst. Solids 549 (2020), https://doi.org/10.1016/j.jnoncrysol.2020.120339.
[29] O. Shpotyuk, M. Hyla, V. Boyko, Structural-topological genesis of network-forming nanoclusters in chalcogenide semiconductor glasses, J Optoelectron Adv Mater 15 (2013) 1429–1437. https://joam.inoe.ro/articles/structural-topological-genesis-of-network-forming-nanoclusters-in-chalcogenide-semiconductor-glasses/fulltext.
[30] O. Shpotyuk, M. Hyla, V. Boyko, Compositionally-dependent structural variations in glassy chalcogenides: The case of binary As-Se system, Comput. Mater. Sci. 110 (2015) 144–151, https://doi.org/10.1016/j.commatsci.2015.08.015.
[31] V. Boyko, M. Hyla, O. Shpotyuk, Chain- and ring-like sulphur clusters: Modelling within HyperChem program, Visnyk Lviv. Univ. Ser. Phys. 43 (2009) 233–237. https://physics.lnu.edu.ua/wp-content/uploads/43_31.pdf.

[32] W.J. Hehre, R.F. Stewart, J.A. Pople, Self-consistent molecular-orbital methods. I. Use of Gaussian expansions of slater-type atomic orbitals, J. Chem. Phys. 51 (6) (1969) 2657–2664, https://doi.org/10.1063/1.1672392.
[33] A.D. McLean, G.S. Chandler, Contracted Gaussian basis sets for molecular calculations. I. Second row atoms, Z=11-18, J. Chem. Phys. 72 (10) (1980) 5639–5648, https://doi.org/10.1063/1.438980.
[34] K. Jackson, Electric fields in electronic structure calculations: electric polarizabilities and IR and Raman spectra from first principles, Phys. Stat. Solidi B 217 (2000) 293–310, https://doi.org/10.1002/(SICI)1521-3951(200001)217:1<293::AID-PSSB293>3.0.CO;2-N.
[35] R. Holomb, M. Veres, V. Mitsa, Ring-, branchy-, and cage-like AsnSm nanoclusters in the structure of amorphous semiconductors: ab initio and Raman study, J. Optoelectron. Adv. Mater. 11 (2009) 917-923. doi: https://dspace.uzhnu.edu.ua/jspui/handle/lib/4320.
[36] O. Shpotyuk, A. Ingram, P. Demchenko, Free volume structure of realgar α-As_4S_4 by positron annihilation lifetime spectroscopy, J. Phys. Chem. Solids 79 (2015) 49–54, https://doi.org/10.1016/j.jpcs.2014.12.001.
[37] O. Shpotyuk, P. Demchenko, Y. Shpotyuk, Z. Bujňáková, P. Baláž, M. Hyla, V. Boyko, Amorphization diversity driven by high-energy mechanical milling in β-As_4S_4 polymorph, 100679–1 11, Mater. Today Commun. 21 (2019), https://doi.org/10.1016/j.mtcomm.2019.100679.
[38] O. Shpotyuk, M. Hyla, V. Boyko, Y. Shpotyuk, V. Balitska, Cluster modeling of amorphization pathways in nanostructured arsenic monosulphide, Appl. Nanosci. (2020), https://doi.org/10.1007/s13204-020-01298-x.
[39] O. Shpotyuk, P. Baláž, Z. Bujňáková, A. Ingram, P. Demchenko, Y. Shpotyuk, Mechanochemically-driven amorphization of nanostructurized arsenicals, the case of β-As_4S_4, J. Mater. Sci. 53 (19) (2018) 13464–13476, https://doi.org/10.1007/s10853-018-2404-3.
[40] P. Baláž, M. Baláž, O. Shpotyuk, P. Demchenko, M. Vlček, M. Shopska, J. Briančin, Z. Bujňáková, Y. Shpotyuk, B. Selepová, Ľ. Balážová, Properties of arsenic sulphide (β-As_4S_4) modified by mechanical activation, J. Mater. Sci. 52 (3) (2017) 1747–1758, https://doi.org/10.1007/s10853-016-0466-7.
[41] O. Shpotyuk, A. Kozdras, P. Baláž, Z. Bujňáková, Y. Shpotyuk, DSC TOPEM® study of high-energy mechanical milling driven amorphization in β-As_4S_4-based arsenicals, J. Therm. Anal. Calorim. 135 (6) (2019) 2935–2941, https://doi.org/10.1007/s10973-018-7613-0.
[42] H.J. Whitfield, The crystal structure of tetra-arsenic trisulphide, J. Chem. Soc. A (1970) 1800–1803, https://doi.org/10.1039/J19700001800.
[43] H.J. Whitfield, Crystal structure of the β-form of tetra-arsenic trisulphide, J. Chem. Soc. Dalton (17) (1973) 1737–1738, https://doi.org/10.1039/DT9730001737.